Frataxin knockin mouse

Carlos J. Miranda[a,b], Manuela M. Santos[a,b], Keiichi Ohshima[a,1], Julie Smith[c], Liangtao Li[c], Michaeline Bunting[c], Mireille Cossée[d], Michael Koenig[d], Jorge Sequeiros[b], Jerry Kaplan[c], Massimo Pandolfo[a,e,*]

[a] *Department of Medicine, Centre Hospitalier de l'Université de Montréal, Hôpital Notre-Dame, Pav de Seve – Y5608, 1560 rue Sherbrooke Est, Montréal, QC, Canada H2L 4M1*
[b] *UnIGENe, IBMC, Universidade do Porto, 4150-180 Porto, Portugal*
[c] *Department of Pathology, School of Medicine, University of Utah, Salt Lake City, UT 84132, USA*
[d] *Institut de Génétique et de Biologie Moléculaire et Cellulaire, CNRS/INSER/Université Louis-Pasteur, C.U. de Strasbourg, 67404 Illkirch, France*
[e] *Service de Neurologie, Hôpital Erasme, 1070 Brussels, Belgium*

Received 18 December 2001; accepted 27 December 2001

First published online 18 January 2002

Edited by Jesus Avila

Abstract Friedreich ataxia is the consequence of frataxin deficiency, most often caused by a GAA repeat expansion in intron 1 of the corresponding gene. Frataxin is a mitochondrial protein involved in iron homeostasis. As an attempt to generate a mouse model of the disease, we introduced a $(GAA)_{230}$ repeat within the mouse frataxin gene by homologous recombination. GAA repeat knockin mice were crossed with frataxin knockout mice to obtain double heterozygous mice expressing 25–36% of wild-type frataxin levels. These mice were viable and did not develop anomalies of motor coordination, iron metabolism or response to iron loading. Repeats were meiotically and mitotically stable.

Key words: Friedreich ataxia; GAA repeat; Frataxin; Knockin mice; Iron metabolism

1. Introduction

Friedreich ataxia (FRDA) is the most common autosomal recessive ataxia in caucasians, with an estimated prevalence of 2–4 per 100 000 individuals [1–3]. The neuropathology in FRDA is characterized by loss of large sensory neurons in the dorsal root ganglia, atrophy of the large sensory fibers in peripheral nerves, of the posterior columns, spinocerebellar and pyramidal tracts in the spinal cord and of the dentate nucleus in the cerebellum [4]. Patients show progressive gait and limb ataxia, dysarthria, lower limbs areflexia, decreased vibration sense, muscle weakness in the legs, and positive extensor plantar responses [5–8]. Most patients also have hypertrophic cardiomyopathy, and about one third have diabetes or carbohydrate intolerance [9–12].

FRDA is typically caused by a large GAA repeat expansion (ranging from 100 to more than 1100 repeats) within the first intron of the gene encoding a protein called frataxin [13]. 96% of patients are homozygous for the GAA repeat expansion, while the remaining are compound heterozygous for a GAA expansion and a point mutation that alters or truncates the coding region of the gene [13,14]. The GAA repeat expansion has been shown to inhibit frataxin transcription [15,16]. Lymphoblastoid cell lines from FRDA patients have a severe reduction in the expression of frataxin, ranging from 4% to 29% of normal levels [17].

Frataxin is a 210 amino acid nuclear-encoded mitochondrial protein that is highly conserved throughout evolution [13,18]. The frataxin homolog in yeast is involved in iron homeostasis, as indicated by the analysis of frataxin knockout yeast (ΔYFH1). YFH1 accumulates 10-fold more iron in mitochondria than wild-type yeast, loses mitochondrial DNA, and is unable to carry out oxidative phosphorylation [19]. The mechanism of mitochondrial iron accumulation is unknown, but the reintroduction of yeast frataxin results in a rapid export of accumulated mitochondrial iron into the cytosol as free, non-heme-bound iron [20]. Several lines of evidence indicate that the function of frataxin is conserved in humans. Work by Cavadini and colleagues has shown that human frataxin cDNA can complement the frataxin-deficient yeast, suggesting that frataxin function is conserved and reinforcing the idea that human frataxin is involved in mitochondrial iron homeostasis [21].

Studies in the mouse have shown that frataxin plays an important role during early embryonic development, since homozygous frataxin knockout mice die in utero shortly after implantation at embryonic day (E)6.5 [22]. In order to develop an animal model for FRDA to investigate the function of frataxin, the mechanism of the disease, and test possible treatments, we generated a knockin mouse that carries a $(GAA)_{230}$ repeat expansion in the first intron of the mouse frataxin homolog gene (*frda*).

2. Materials and methods

2.1. Construction of the targeting vector

A cloned *Bam*HI–*Bgl*II fragment from intron 1 of the frataxin gene, containing a $(GAA)_{230}$ repeat and a flanking sequence of 350 bp upstream and 250 bp downstream, was obtained as described in [16]. This fragment was inserted in the *Xba*I/*Bsi*Iw site of the MFneoTK vector, which contains a phosphoglycerate kinase promoter/neomycin resistance gene cassette, flanked by loxP sites in the same orientation as the GAA repeat. This MFNeoTKGAA230 construct was then cloned into the first intron of the *frda* gene, which was contained in

*Corresponding author. Fax: (1)-514-412 7661.
E-mail address: massimo.pandolfo@ulb.ac.be (M. Pandolfo).

[1] Present address: Growth Factor Division, National Cancer Center Research Institute, Tokyo 104-0045, Japan.

0014-5793/02/$22.00
PII: S0014-5793(02)02251-2

a cosmid clone along with the first and second exon of the gene. The complete construct was introduced into *Escherichia coli* DH5α by electroporation.

2.2. Gene targeting in ES cells and generation of chimeras

Following linearization at the unique *Sal*I site, the targeting vector was electroporated into 129/Sv ES cells grown on feeder layers. After G418 selection, the DNA of resistant clones was analyzed by PCR using primers GAA-F and GAA-R [13]. To generate chimeras, targeted ES cells were injected into C57BL/6J host blastocysts, which were then transferred into pseudo-pregnant females. Male chimeras were selected by coat color and crossed with C57BL/6J females to obtain germline transmission of the targeted *frda*^{230GAA} allele.

2.3. Animals

The Institutional Animal Care Committee reviewed and approved all procedures performed in accordance with the Canadian Council on Animal Care guidelines. Frataxin heterozygous knockin mice (*frda*$^{+/230GAA}$) were crossed to generate frataxin homozygous knockin mice (*frda*$^{230/230GAA}$). To further decrease frataxin expression, frataxin heterozygous knockout mice (*frda*$^{+/-}$) [22] were crossed with *frda*$^{+/230GAA}$ mice, to generate frataxin knockout/knockin mice (*frda*$^{-/230GAA}$).

2.4. Genotype analysis

Genomic DNA was prepared from tail biopsies. Mouse genotyping included a set of two multiplex PCRs specific for the knockout and knockin *frda* loci. The multiplex PCR for genotyping the knockin allele includes a common forward primer (P1: 5′-TTAGACAGA-CATGCACAAACAGAAT-3′) and two reverse primers specific for the wild-type (P2: 5′-TGT GGG TGA CCT TGG AGG GAG-3′) and knockin (P3: 5′-CCT AAC TTT TAA GCA CTG GCA AC-3′) *frda* alleles. PCR products are 313 bp for the wild-type allele and 230 bp for the knockin allele (Fig. 1B). The multiplex PCR for genotyping the *frda* knockout allele includes a common forward primer (WJ5: 5′-CTGTTTACCATGGCTGAGATCTC-3′) and two reverse primers specific for the wild-type (WN39: 5′-CCA AGG ATA TAA CAG ACA CCA TT-3′) and knockout (WC76: 5′-CGC CTC CCC TAC CCG GTA GAA TTC-3′) *frda* alleles [22]. The PCR products are 520 bp for the wild-type allele and 245 bp for the knockout allele (Fig. 1C).

2.5. Quantification of frataxin expression by PCR LightCycler

Dissected mouse hearts were immediately extracted for RNA using the Trizol reagent (Gibco BRL, Rockville, MD, USA). cDNA synthesis was performed as described [34]. RNA (5 μg) was converted to cDNA using M-MuLV-RTase (Gibco BRL) at 37°C for 1 h. The cDNA samples were digested with RNase A for 2 min and followed by Qiagen purification column. PCR was performed in a LightCycler from Roche Molecular Biochemicals. The two primers used for amplification were: 5′-GCC CAT TTG AAC CTC CAC TAC C-3′ and 5′-CTT GTT TGG GGT CTG CTT GTT G-3′. Sybergreen I (Molecular Probe, Eugene, OR, USA) was used as a fluorescence indicator. A total of 40 cycles were run under the following conditions: denaturing 95°C, 1 s; annealing 57°C, 1 s; elongation 72°C, 10 s. The melting cycle was performed as 95°C (1 s), 40°C (20 s), 95°C (1 s). The PCR quantification was normalized by internal control β-actin. The frataxin expression level was reported as percentage to wild-type mice.

2.6. Western blot analysis

Tissues were homogenized in 10 volumes of Laemmli buffer and

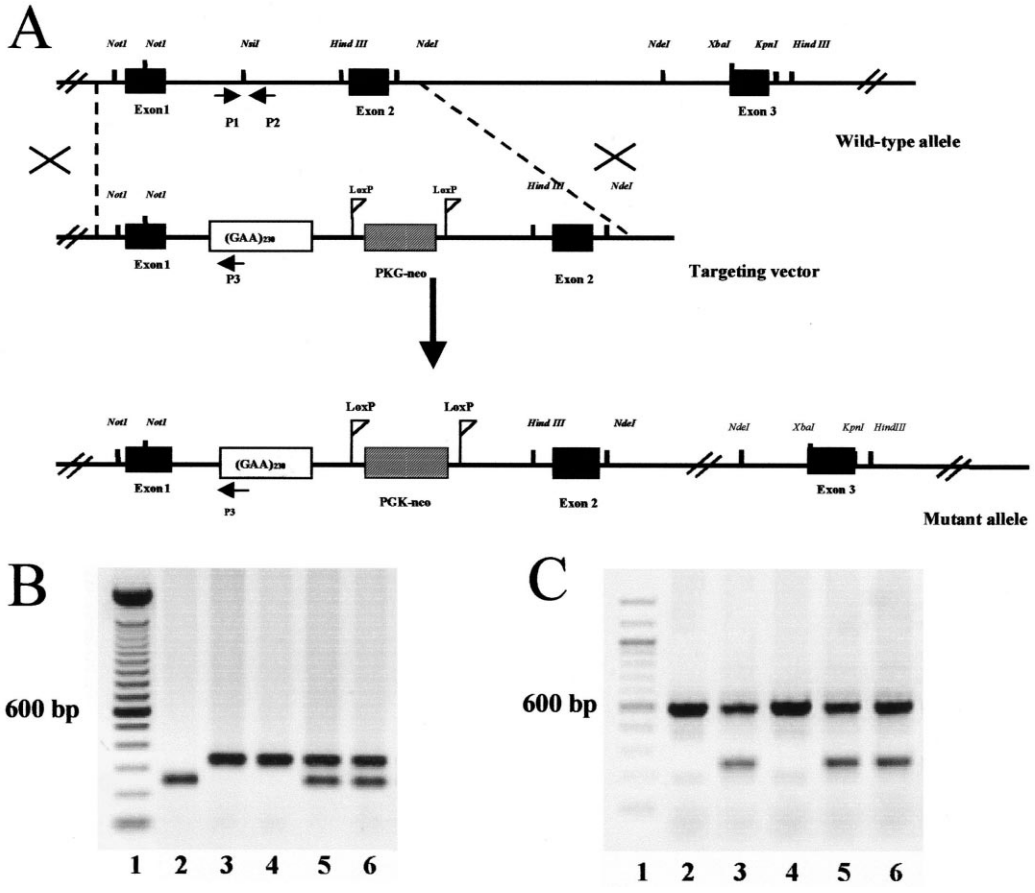

Fig. 1. A: Targeting strategy for the insertion of a $(GAA)_{230}$ repeat expansion into intron 1 of the mouse frataxin gene. The genomic structure of the wild-type locus encompassing exon 1–3 (black boxes) is depicted at the top. The targeting plasmid is represented in the middle. P1–P3, primers used for genotyping mouse DNA by multiplex PCR. B: PCR analysis for detection of frataxin knockin allele. C: PCR analysis for detection of frataxin knockout allele. Lane 1: ladder 100 bp; lane 2: *frda*$^{230/230GAA}$; lane 3: *frda*$^{+/-}$; lane 4: wild-type; lanes 5 and 6: *frda*$^{-/230GAA}$.

adjusted to a final protein concentration of 15 μg/μl, using the Sigma protein assay following the manufacturer's protocol (Sigma, St. Louis, MO, USA). 20 μg of each homogenate were loaded onto a 12% Tris–glycine sodium dodecyl sulfate (SDS)–polyacrylamide gel, run by electrophoresis and then blotted onto a Hybond-C super (Amersham-Life Science, Arlington Heights, IL, USA) membrane. Blots were probed with a monoclonal antibody to frataxin (Chemicon, Temecula, CA, USA) as well as a monoclonal antiserum to β-tubulin (Calbiochem, San Diego, CA, USA) to compare protein concentration for each sample. Specific signals were visualized by chemiluminescence. Quantification of frataxin expression was determined by analyzing autoradiograms with Scion imager software (Scion Corporation, MD, USA). The intensity of each frataxin band was corrected according to the intensity of the β-tubulin band for that same lane. Wild-type and frataxin knockout heterozygous mice were used as controls for the amount of frataxin.

2.7. Serum iron and transferrin saturation

Blood was collected by heart puncture under pentobarbital anesthesia, and serum was separated. Serum iron and total iron-binding capacity were determined by a colorimetric assay using a Kodak Ektachem DT60 instrument (Johnson&Johnson, Clinical Diagnostics).

2.8. Diets

Dietary iron loading was obtained by placing 6-week-old mice on an iron-enriched diet containing 3% (w/w) carbonyl–iron (Sigma, St. Louis, MO, USA), for a period of 2 months. To induce parenteral iron loading, 5 mg of iron–dextran (Sigma) were injected i.p., three times per week, for a total amount of 85 mg/mouse, during a period of 2 months.

2.9. Measurement of tissue iron levels

Organ samples were weighed wet, then dried overnight at 106°C and weighed again. The dried samples were ashed in an oven at 500°C for 17 h, solubilized in 6 N HCl, and the final solution was adjusted with demineralized water to a final concentration of 1.2 mol/l. Iron concentration was determined by flame atomic absorption spectrometry.

2.10. Size of GAA repeat

To determine the size of the GAA repeat, fragments were amplified using the primers GAA-F2 (5′-GAT CAC CTG AGG TCC GGA GTT CAA GAC T-3′) and GAAR-R2 (5′-GAT TCT CCT GCC GCA GCC TCT GGA GTA GC-3′). The PCR products were run overnight in a 0.8% agarose gel at 40 V. The expected fragment size is 890 bp.

2.11. Histology

Tissue samples from liver, spleen, heart and pancreas were fixed in buffered 4% formaldehyde and embedded in paraffin. Tissue sections were stained with hematoxilin/eosin and trichrome blue for demonstration of fibrosis. Ferric iron (Fe(III)) was detected by Prussian blue staining.

2.12. Rotarod analysis

Motor coordination and balance were assessed using an accelerating rotarod apparatus (Stoelting Co, Wood Dale, IL, USA). Mice were trained in four trials (T1–T4) per day for 4 consecutive days (D1–D4). Each trial lasted a maximum of 10 min, during which time the rotating rod accelerates from 4 to 40 rpm over the first 5 min of the trial and was then held at maximum speed for the remaining 5 min. A minimum of 10 min between trials was allowed to avoid animal fatigue and exhaustion.

3. Results

3.1. Generation of frataxin knockin mice

The major cause of FRDA is the presence in homozygosity of a large GAA repeat expansion in the first intron of the frataxin gene, that decreases frataxin expression to less than 30% of normal levels [17]. With the aim to generate an animal model showing a reduction in frataxin expression similar to FRDA patients, we generated a frataxin knockin mouse by targeting a GAA repeat expansion to intron 1 of the mouse frataxin gene. A fragment containing a $(GAA)_{230}$ repeat expansion, originally cloned from a FRDA patient, was inserted in the mouse genome by homologous recombination (Fig. 1A). Male chimeras were selected by coat color and crossed with C57BL/6J females to obtain germline transmission of the targeted *frda*^{230GAA} allele.

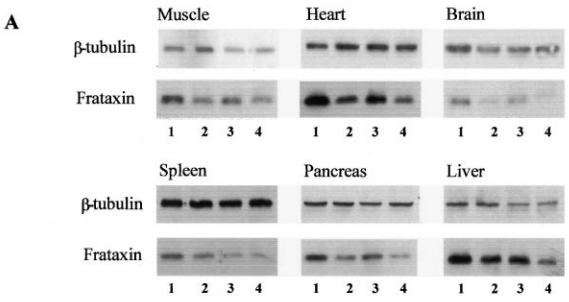

Levels of frataxin compared with wild-type mice (%)

Mouse	Heart	Liver	Spleen	Pancreas	Brain	Muscle
Frda$^{-/230GAA}$	28 ± 8	27 ± 4	36 ± 9	32 ± 3	25 ± 4	25 ± 1
Frda$^{230/230GAA}$	76 ± 7	83 ± 4	71±5	82 ± 15	66 ± 7	83 ± 5

Data are presented as means ± SD

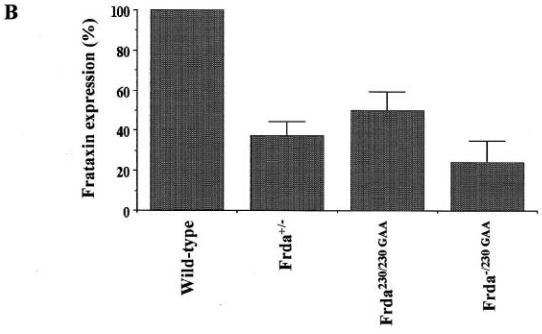

Fig. 2. Frataxin levels are reduced in homozygous frataxin knockin and in knockin/knockout mice, when compared to wild-type mice. A: Total protein extract (20 μg) from mouse tissues was immunoblotted with frataxin and β-tubulin antibodies. Lane 1, wild-type; lane 2, *frda*$^{+/-}$; lane 3, *frda*$^{230/230GAA}$; lane 4, *frda*$^{-/230GAA}$. Densitometric analysis of frataxin protein expression is shown below. B: Total RNAs were isolated from the hearts of wild-type and mutant mice, and RT-PCR was carried out with frataxin-specific primers. The PCR quantification was normalized by internal control -actin. The frataxin expression levels are reported as percentage to wild-type mice.

3.2. Frataxin levels in frataxin knockin/knockout mice

Levels of frataxin expression in skeletal muscle, heart, brain, spleen, pancreas, and liver of both knockin and knockin/knockout mice were analyzed by Western blot (Fig. 2A). Densitometric analysis of Western blots indicates that the presence of a $(GAA)_{230}$ repeat in homozygous frataxin knockin mice (*frda*$^{230/230GAA}$) leads to a reduction in the levels of frataxin expression in all tissues examined, averaging 75% of wild-type levels. Nevertheless, these values of frataxin expression were still too high to expect the mice to develop a FRDA-like phenotype, since frataxin knockout mice (*frda*$^{+/-}$), which have approximately 50% of frataxin levels

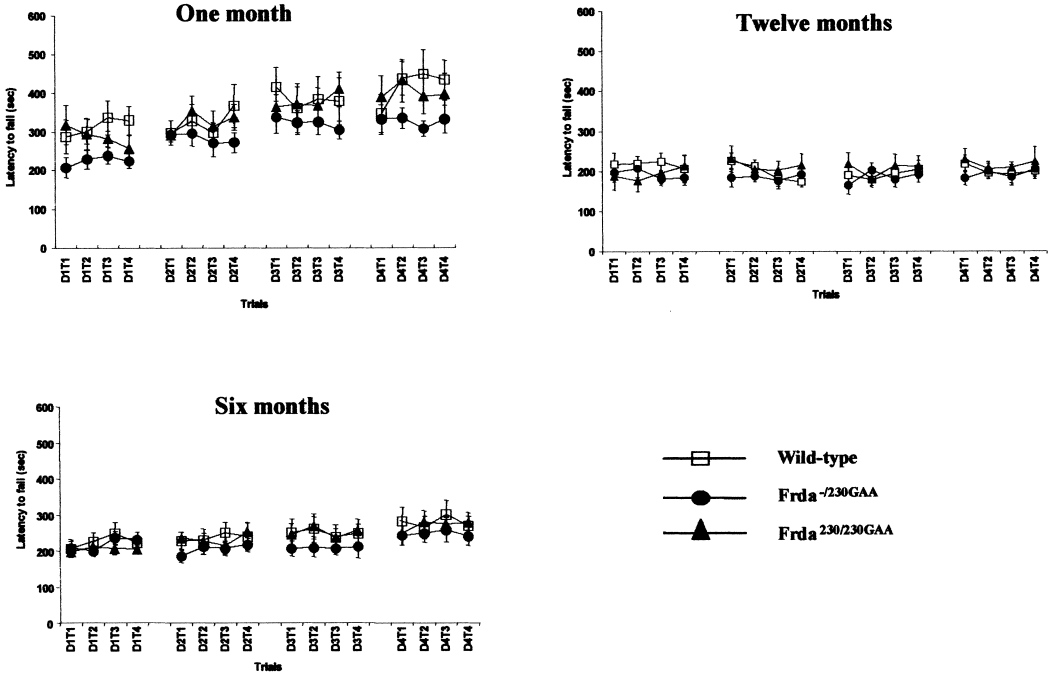

Fig. 3. Motor coordination in *frda*$^{230/230GAA}$ and *frda*$^{-/230GAA}$ mice is indistinguishable from wild-type littermates, as evaluated by the accelerating rotarod. Data are presented as means ± S.E.M.

when compared to wild-type mice are phenotypically indistinguishable from their control littermates [23]. In order to further decrease frataxin levels, we crossed frataxin knockin mice with *frda*$^{+/-}$ mice, thus generating knockin/knockout mice (*frda*$^{-/230GAA}$). Analysis of frataxin expression in tissues from *frda*$^{-/230GAA}$ mice shows a reduction of frataxin to 25 to 36% of wild-type mice levels (Fig. 2). This value lies within the range of expression reported in mildly affected FRDA patients [17].

3.3. Characterization of frataxin knockin/knockout mice

Clinical features in FRDA patients include uncoordinated gait and limb movements (ataxia), diminished or absent tendon reflexes, and impairment of proprioreception and balance. We investigated *frda*$^{-/230GAA}$ mice for FRDA-like symptoms by testing their motor coordination and balance using an accelerating rotarod apparatus. Tests were performed every 3 months starting at the age of 1 month (Fig. 3). Since symptoms in humans appear progressively, we followed these mice over a period of 1 year. *Frda*$^{-/230GAA}$ mice performed similarly as the wild-type mice on the rotarod, up to the age of 1 year.

Frataxin affects iron homeostasis in mitochondria [19,21], therefore we analyzed iron metabolism in *frda*$^{-/230GAA}$ mice. Levels of serum iron, transferrin saturation, and tissue iron concentration were determined in 1-year-old mice. Serum iron and transferrin were in the normal range (data not shown). Total iron concentration in tissues were similar in *frda*$^{-/230GAA}$ mice and their wild-type littermates (Table 1), except in pancreas, where iron levels were lower in *frda*$^{-/230GAA}$ mice ($P < 0.01$).

The heart is affected in the vast majority of FRDA patients [9,14,24] and shows intracellular iron deposits in cardiomyocytes [25] related to heart fibrosis. We analyzed heart samples from 1-year-old *frda*$^{-/230GAA}$ mice for the presence of iron and collagen deposition. No iron deposits and only mild collagen staining, especially around vessels, were observed in both *frda*$^{-/230GAA}$ and wild-type mice.

One out of twelve *frda*$^{+/-}$ mice, and two out of 13 *frda*$^{-/230GAA}$ mice died during the time course of the experiment. No deaths were recorded in wild-type and *frda*$^{230/230GAA}$ mice during the same period of time. Interestingly, one *frda*$^{-/230GAA}$ mouse that died at the age of 12 months had levels of iron in the heart almost three times higher than its littermates (1168 μg, average 399 μg Fe/g dry weight), and prominent heart fibrosis.

3.4. Effect of iron challenge in frataxin double heterozygous mice

We next studied the response of *frda*$^{-/230GAA}$ mice to iron

Table 1
Tissue iron concentration

Mice	*n*	Liver	Heart	Pancreas	Spleen
		μg Fe/g dry weight			
frda$^{+/+}$	8	227 ± 59	412 ± 85	175 ± 24	3048 ± 1438
frda$^{+/-}$	12	292 ± 84	372 ± 28	183 ± 43	1741 ± 669*
frda$^{230/230\ GAA}$	9	247 ± 72	431 ± 56	159 ± 75	3206 ± 1339
frda$^{-/230\ GAA}$	13	223 ± 74	399 ± 67	141 ± 22**	2034 ± 801

Data are presented as mean ± S.D. *n*, number of animals. Student's *t*-test was used for comparison with wild-type mice (*$P < 0.05$; **$P < 0.01$).

Table 2
Tissue iron concentration

Treatment	*n*	Liver	Heart	Pancreas	Spleen
		μg Fe/g dry weight			
–	8	258 ± 69	445 ± 41	143 ± 22	1960 ± 1091
CI	6	1840 ± 1045***	455 ± 21	175 ± 26*	6281 ± 2794**
Fe-Dex	6	22309 ± 3557†	4107 ± 981†	4703 ± 1951†	23407 ± 4883†

CI: carbonyl–iron-enriched diet; Fe-dex: iron–dextran treatment. Data are presented as mean ± S.D. *n*, number of animals. Student's *t*-test was used for comparison between untreated and treated mice (*$P < 0.05$; **$P < 0.01$; ***$P < 0.001$; †$P < 0.0001$).

challenge. Iron loading was obtained either by i.p. injection of iron–dextran (85 mg/kg total), or by supplementing their diet with carbonyl–iron (3% w/w) for a 2-month period. These two iron loading methods affect different cell types [26]. In the liver, iron–dextran leads to iron accumulation predominantly in Kupffer and endothelial cells, while carbonyl–iron supplementation leads to iron accumulation predominantly in hepatocytes, and moderately in Kupffer cells. Both treatments result in a statistically significant increase in iron concentration, as determined by flame atomic absorption spectrometry, in all organs, with the exception of the heart in carbonyl–iron-supplemented mice (Table 2). Since FRDA patients often show fibrosis in cardiac tissue, we analyzed the hearts of *frda*$^{-/230GAA}$ mice for fibrosis using trichrome blue staining. Despite the remarkably high levels of tissue iron accumulation in the heart of iron–dextran-treated mice, collagen was practically undetectable (data not shown). Carbonyl–iron-supplemented diet also did not result in significant cardiac collagen deposition (data not shown). In order to determine whether these iron loading conditions had an effect on the nervous system and could trigger ataxia in *frda*$^{-/230GAA}$ mice, motor coordination was assessed by rotarod. *Frda*$^{-/230GAA}$ mice performed similarly to the wild-type animals (Fig. 4).

3.5. Stability of the *frda*^{230GAA} allele

Large GAA repeat expansions are unstably transmitted from parent to offspring, and show somatic instability in FRDA patients [27–30]. We investigated intergenerational GAA repeat transmission in *frda*$^{-/230GAA}$ and *frda*$^{230/230GAA}$ mice by comparing the length of the repeat in each parent with that observed in their progeny. No detectable change in the GAA repeat size was found over the six studied generations (Fig. 5A). Furthermore, the GAA repeat expansion size was the same in all analyzed tissues (Fig. 5B).

4. Discussion

The major cause of FRDA is the presence in homozygosity of a large GAA repeat expansion in intron 1 of the frataxin gene that decreases the level of frataxin expression. Experiments using in vitro and in vivo systems revealed that the GAA repeat interferes with transcription in an orientation- and length-dependent manner [15,16,31]. The molecular basis of this mechanism lead to the discovery of a novel DNA structure that has been designated sticky DNA [32]. Large GAA repeats lead to greater reductions in frataxin expression, which correlate with a more severe phenotype and an earlier age of onset. No mutations leading to a complete loss of frataxin expression have been reported in humans, suggesting that total frataxin deficiency may be incompatible with life. This was confirmed by the observation that homozygous frataxin knockout mice die in utero shortly after implantation (E6.5) [22].

In order to establish an animal model for FRDA that mirrors the chronically reduced levels of frataxin expression found in the human disease, we generated a knockin mouse model that carries a $(GAA)_{230}$ repeat in the *frda* gene. This repeat, when in homozygosity, only leads to a decrease in frataxin expression to 75% of wild-type levels. We further decreased frataxin expression by generating frataxin knockin/knockout mice (*frda*$^{-/230GAA}$) which show approximately 25–30% of frataxin levels compared to wild-type. This level of frataxin is compatible with a normal embryonic development and is associated with mild, but clinically evident FRDA

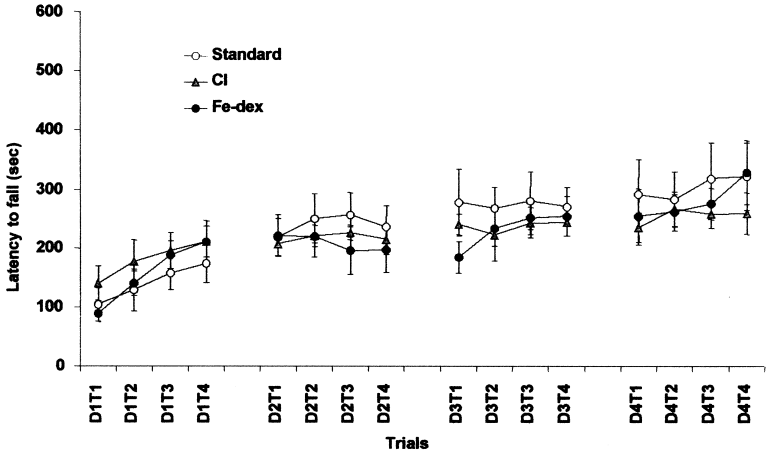

Fig. 4. Effect of iron loading in frataxin knockout/knockin mice-rotarod analysis.

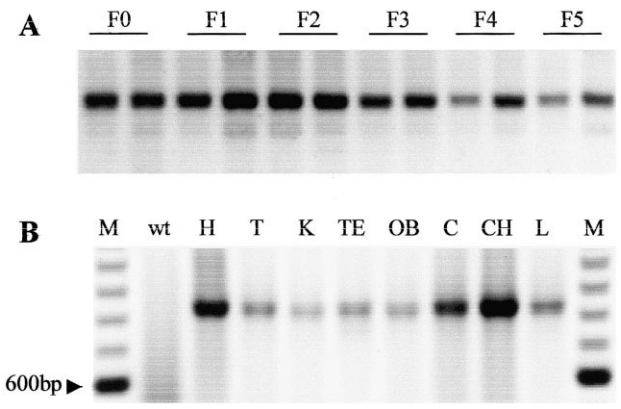

Fig. 5. Stability of the (GAA)230 repeat inserted in the mouse genome was shown during parent–offspring transmission, and in somatic tissues. A: PCR analysis of the GAA repeat size during parent–offspring transmission in *frda*$^{-/230GAA}$ mice. B: PCR analysis of the GAA repeat size in somatic tissues of *frda*$^{-/230}$GAA mice. F0–F5, mouse generation number. M, ladder 100 bp; wt, control wild-type; H, heart; T, tail; K, kidney; TE, testis; OB, olfactory bulbs; C, cerebellum; CH, cerebellar hemisphere, L, liver.

in humans. We therefore analyzed *frda*$^{-/230GAA}$ mice for signs of ataxia and cardiomyopathy. Rotarod analysis performed up to the age of one year old did not reveal any motor incoordination in *frda*$^{-/230GAA}$ mice. The hearts of *frda*$^{-/230GAA}$ mice were negative for iron staining. Thus, 25–30% of wild-type frataxin levels seems to be compatible with normal neurological function and iron metabolism in mice.

We studied the response of *frda*$^{-/230GAA}$ mice to challenge with iron–dextran or carbonyl–iron and found that it did not differ from the response of wild-type mice. Furthermore, iron overload did not lead to significant cardiac fibrosis. These data indicate that iron per se does not trigger ataxia, nor heart damage in mice expressing some residual frataxin. A recent FRDA mouse model, in which frataxin is conditionally knocked out in cardiac and skeletal muscle, develops cardiomyopathy with intramitochondrial iron deposits specifically in cardiomyocytes. However, these deposits only appear after other biochemical markers of mitochondrial dysfunction, particularly reduced activities of iron–sulfur enzymes, suggesting that gross iron accumulation is a late event even in complete frataxin deficiency [33].

GAA repeat instability has been reported to occur during parent to offspring transmission and in somatic tissues of FRDA patients [27–30]. We investigated intergenerational GAA repeat transmission and the length of the repeat in somatic tissues in *frda*$^{-/230GAA}$ and *frda*$^{230/230GAA}$ mice. We found out that, in our mouse model, a $(GAA)_{230}$ repeat is meiotically and mitotically stable. In humans, such a repeat is moderately unstable, so that several easily detectable changes in size would have been identified in a similar number of transmission events.

In summary, our study shows that: (1) low levels of frataxin expression close to 25–30% of wild-type levels are not associated with any obvious pathological phenotype in mice; (2) GAA repeat lengths that are unstable in humans are meiotically and mitotically stable in the mouse strain we investigated.

Acknowledgements: This work was supported by Canadian Institutes of Health Research (CIHR, Grant no FRN14689) to M.P., the National Institutes of Health Grant (NIH, NIDDK, Grant 52380) to J.K. and the Fundação para a Ciência e a Tecnologia (FCT, Grant POCTI/34535/MGI/2000) to J.Se. J.Sm. was supported by a NIH training Grant (T32-NIDDK 07115). C.J.M. and M.M.S. were supported by a Scholarship from FCT (PRAXIS XXI/BD/16249/98 and PRAXIS XXI/BPD/18833/98).

References

[1] Romeo, G., Menozzi, P., Ferlini, A., Fadda, S., Di Donato, S., Uziel, G., Lucci, B., Capodaglio, L., Filla, A. and Campanella, G. (1983) Am. J. Hum. Genet. 35, 523–529.
[2] Leone, M., Brignolio, F., Rosso, M.G., Curtoni, E.S., Moroni, A., Tribolo, A. and Schiffer, D. (1990) Clin. Genet. 38, 161–169.
[3] Cossée, M., Schmitt, M., Campuzano, V., Reutenauer, L., Moutou, C., Mandel, J-L. and Koenig, M. (1997) Proc. Natl. Acad. Sci. USA 94, 7452–7457.
[4] Pandolfo, M. and Koenig, M. (1998) in: Genetic instabilities and hereditary neurological diseases (Wells, R.D. and Warren, S.T., Eds.), Academic press, London.
[5] Geoffroy, G., Barbeau, A., Breton, G., Lemieux, B., Aube, M., Leger, C. and Bouchard, J.P. (1976) Can. J. Neurol. Sci. 3, 279–286.
[6] Harding, A.E. (1981) Brain 104, 589–620.
[7] Pentland, B. and Fox, K.A. (1983) J. Neurol. Neurosurg. Psychiatry 46, 1138–1142.
[8] Harding, A.E. (1983) Lancet 1, 1151–1155.
[9] Dürr, A., Cossée, M., Agid, Y., Campuzano, V., Mignard, C., Penet, C., Mandel, J-L., Brice, A. and Koenig, M. (1996) New. Engl. J. Med. 335, 1169–1175.
[10] Filla, A., De Michele, G., Cavalcanti, F., Pianese, L., Monticelli, A., Campanella, G. and Cocozza, S. (1996) Am. J. Hum. Genet. 59, 554–560.
[11] Montermini, L., Richter, A., Morgan, K., Justice, C.M., Julien, D., Castellotti, B., Mercier, J., Poirier, J., Capozzoli, F., Bouchard, J.P., Lemieux, B., Mathieu, J., Vanasse, M., Seni, M.H., Graham, G. and Pandolfo, M. (1997) Ann. Neurol. 41, 675–682.
[12] Monros, E., Molto, M.D., Martinez, F., Canizares, J., Blanca, J., Vilchez, J.J., Prieto, F., De Frutos, R. and Palau, F. (1997) Am. J. Hum. Genet. 61, 101–110.
[13] Campuzano, V., Montermini, L., Moltó, M.D., Pianese, L., Cossée, M., Cavalcanti, F., Monros, E., Rodius, F., Duclos, F. and Monticelli, A. et al. Friedreichs ataxia: autosomal recessive disease caused by an intronic GAA triplet repeat expansion, (1996) Science 271, 1423–1427.
[14] Cossée, M., Durr, A., Schmitt, M., Dahl, N., Trouillas, P., Allinson, P., Kostrzewa, M., Nivelon-Chevallier, A., Gustavson, K.H., Kohlschutter, A., Muller, U., Mandel, J.L., Brice, A., Koenig, M., Cavalcanti, F., Tammaro, A., De Michele, G., Filla, A., Cocozza, S., Labuda, M., Montermini, L., Poirier, J. and Pandolfo, M. (1999) Ann. Neurol. 45, 200–206.
[15] Bidichandani, S.I., Ashizawa, T. and Patel, P.I. (1998) Am. J. Hum. Genet. 62, 111–121.
[16] Ohshima, K., Montermini, L., Wells, R.D. and Pandolfo, M. (1998) J. Biol. Chem. 273, 14588–14595.
[17] Campuzano, V., Montermini, L., Lutz, Y., Cova, L., Hindelang, C., Jiralerspong, S., Trottier, Y., Kish, S.J., Faucheux, B., Trouillas, P., Authier, F.J., Durr, A., Mandel, J-M., Vescovi, A., Pandolfo, M. and Koenig, M. (1997) Hum. Mol. Genet. 6, 1771–1780.
[18] Koutnikova, H., Campuzano, V., Foury, F., Dolle, P., Cazzalini, O. and Koenig, M. (1997) Nat. Genet. 16, 345–351.
[19] Babcock, M., De Silva, D., Oaks, R., Davis-Kaplan, S., Jiralerspong, S., Montermini, L., Pandolfo, M. and Kaplan, J. (1997) Science 276, 1709–1712.
[20] Radisky, D.C., Babcock, M.C. and Kaplan, J. (1999) J. Biol. Chem. 274, 4497–4499.
[21] Cavadini, P., Gellera, C., Patel, P.I. and Isaya, G. (2000) Hum. Mol. Genet. 9, 2523–2530.
[22] Cossée, M., Puccio, H., Gansmuller, A., Koutnikova, H., Dierich, A., LeMeur, M. and Fishbeck, K. (2000) Hum. Mol. Genet. 9, 1219–1226.

[23] Santos, M.M., Miranda, C.J., Levy, J.J., Montross, L.K., Cossée, M., Sequeiros, J., Andrews, N., Koenig, M. and Pandolfo, M. (2001) Lab. Invest., submitted.
[24] Delatycki, M.B., Williamson, R. and Forrest, S.M. (2000) J. Med. Genet. 37, 1–8.
[25] Lamarche, J.B., Shapcott, D., Côté, M., and Lemieux, B. (1993) in: Handbook of cerebellar diseases′ (Lechtenberg, R., Ed.), pp 453–458, Marcel Dekker, New York.
[26] Santos, M., Clevers, H., De Sousa, M. and Marx, J.J. (1998) Blood 91, 3059–3065.
[27] Montermini, L., Kish, S.J., Jiralerspong, S., Lamarche, J.B. and Pandolfo, M. (1997) Neurology 49, 606–610.
[28] Montermini, L., Andermann, E., Labuda, M., Richter, A., Pandolfo, M., Cavalcanti, F., Pianese, L., Iodice, L., Farina, G., Monticelli, A., Turano, M., Filla, A., De Michele, G. and Cocozza, S. (1997) Hum. Mol. Genet. 6, 1261–1266.
[29] De Michele, G., Cavalcanti, F., Criscuolo, C., Pianese, L., Monticelli, A., Filla, A. and Cocozza, S. (1998) Hum. Mol. Genet. 7, 1901–1906.
[30] Bidichandani, S.I., Purandare, S.M., Taylor, E.E., Gumin, G., Machkhas, H., Harati, Y., Gibbs, R.A., Ashizawa, T. and Patel, P.I. (1999) Hum. Mol. Genet. 8, 2425–2436.
[31] Ohshima, K., Sakamoto, N., Labuda, M., Poirier, J., Moseley, M.L., Montermini, L., Ranum, L.P., Wells, R.D. and Pandolfo, M. (1999) Neurology 53, 1854–1857.
[32] Sakamoto, N., Chastain, P.D., Parniewski, P., Ohshima, K., Pandolfo, M., Griffith, J.D. and Wells, R.D. (1999) Mol. Cell 3, 465–475.
[33] Puccio, H., Simon, D., Cossée, M., Criqui-Filipe, P., Tiziano, F., Melki, J., Hindelang, C., Matyas, R., Rustin, P. and Koenig, M. (2001) Nat. Genet. 27, 181–186.
[34] Tan, S.S. and Weis, J.H. (1992) PCR Methods Appl. 2, 137–143.